The Geological Society of America
Special Paper 557

Fluid-assisted brecciation of Lower Cretaceous Maiolica limestone in the Umbria-Marche Apennines: Hydrodynamical implications

Lung Sang Chan*
HKU SPACE Community College, and Department of Earth Sciences, The University of Hong Kong, Pokfulam Road, Hong Kong

Walter Alvarez
Department of Earth and Planetary Sciences, University of California, Berkeley, California 94707, USA, and *Osservatorio Geologico di Coldigioco, Contrada Coldigioco 62021, Apiro, Italy*

Peter Geiser
G-O-Image LLC., 150 River Way, Lyons, Colorado 80540, USA

Enrico Tavarnelli
Dipartimento di Scienze Fisiche, della Terra e dell'Ambiente, Università di Siena, 53100 Siena, Italy

ABSTRACT

The formation of the "expansion breccia" observed in the Lower Cretaceous Maiolica limestone in the Umbria-Marches region of Italy is attributable to a fluid-assisted brecciation process that occurred during the late Miocene exhumation of the Northern Apennines. The hydrothermal fluids probably originated as brine solutions trapped in the Burano anhydrite while it was in a plastic state. The migration of the Burano from the plastic to the brittle domain during unroofing resulted in liberation and injection of over-pressured hydrothermal fluids into the overlying limestone, causing hydraulic fracturing. Mapping of breccia morphology along a 400-m transect showed structures produced by different flow regimes, with chaotic and mosaic breccia characterizing the core parts of the section and mineral-filled fractures and veins in the margins. Based on the clast size in the chaotic breccia, the estimated velocities for fluidizing the aggregates of clasts and sustaining the clasts in suspension are, respectively, 15 cm/s and 65 cm/s. Crack growth was probably the main mechanism for the fragmentation of the limestone. Explosion fracturing patterns were only sporadically observed in the breccia, indicating substantial heat loss of the over-pressured fluids during their ascent to the Earth's surface.

*chanls@hku.hk

Chan, L.S., Alvarez, W., Geiser, P., and Tavarnelli, E., 2022, Fluid-assisted brecciation of Lower Cretaceous Maiolica limestone in the Umbria-Marche Apennines: Hydrodynamical implications, *in* Koeberl, C., Claeys, P., and Montanari, A., eds., From the Guajira Desert to the Apennines, and from Mediterranean Microplates to the Mexican Killer Asteroid: Honoring the Career of Walter Alvarez: Geological Society of America Special Paper 557, p. 99–114, https://doi.org/10.1130/2022.2557(07).

INTRODUCTION

Breccia can occur in a wide variety of geological settings. Breccia layers concordant with a stratigraphic sequence are generally the products of sedimentological or volcanic processes. Discordant and incoherent breccia bodies, on the other hand, are often the results of karst collapse, tectonic faulting, or hydrothermal fluid injection. In recent years, the process of fluid-assisted brecciation has received much attention from geologists and geophysicists (Sibson, 1996; Jébrak, 1997; Clark and James, 2003; Shukla and Sharma, 2018; Peacock et al., 2019). For the geophysicist, brecciation reveals information on the role played by lithospheric fluids in triggering fault motions and earthquakes. The size and morphology of the clasts, as well as the clast-matrix-void ratios of a breccia can provide information on the kinematics of the fault motion and the hydrodynamic processes leading to the brecciation. Economic geologists are interested in breccias formed in hydrothermal environments, because these breccias are commonly associated with metallic ore deposits (e.g., Kalliokoski and Rehn, 1987; Scheepers and Cuney, 1992; Jébrak et al., 1996; Fournier, 1999; Tămaș and Milési, 2002; Zhang et al., 2007; Costa et al., 2014; Sutarto et al., 2015; Grare et al., 2018; Müller et al., 2018). The formations of low- and high-sulphidation ores, as well as the concentration of gold and other metallic ores, around a magmatic body are reported to be controlled by hydraulic condition of the phreatomagmatic processes (see John et al., 2018, for a detailed summary). While fluid-assisted brecciation can occur in compressional, extensional, and strike-slip settings (Peacock et al., 2019), breccias formed in amagmatic ways, especially those lacking metallic mineralization, are a relatively little studied topic.

Earlier papers described in detail the field observations and geochemistry of breccia in the Lower Cretaceous Maiolica limestone at several localities in the Umbria-Marches region of the Northern Apennines, Italy (Alvarez et al., 2019; Belza et al., 2019; Fig. 1, modified from Alvarez et al., 2019, fig. 1.). The term "expansion breccia" was used for these rocks, because they gave evidence of expansion in all directions, as if the brecciation did not involve the presence of any deviatoric stresses. The breccia is not associated with any known magmatism or metallogenesis of the region. Unlike most hydrothermal breccias with cracks and veins filled by secondary silica, the breccia matrix is primarily sparry calcite, suggesting the involvement of supercritical CO_2 in the precipitation process (Alvarez et al., 2016). The brecciation evidently formed by hydraulic fracturing of the limestone followed by rapid precipitation of calcite in the fractures. We conclude below that fluid-assisted brecciation was probably caused by sudden changes in subsurface physical environment resulting from breaching of over-pressured fluid traps in certain stratigraphic units.

The present paper discusses the hydrodynamical implications of the Maiolica breccia and proposes a model for its formation. We draw on studies of fluid-assisted brecciation in other parts of the world that are relevant to the formation of the Maiolica breccia and consider the hydrodynamic implications of the structural characteristics of the breccia. Specifically, this paper complements the earlier reports of Alvarez et al. (2016, 2019) and Belza et al. (2019) by presenting discussions about (1) the fluid-flow dynamics associated with the formation of the Maiolica breccia, (2) the P-T path of the over-pressured fluids from observed fracturing patterns, and (3) a model for brecciation in the context of the regional geology and stratigraphy.

CLASSIFICATION OF BRECCIAS

Breccia is a rock consisting of broken fragments embedded in a matrix of fine-grained particles or a cement of secondary minerals. Breccias develop in the brittle domain of the crust, when applied stress is greater than the elastic strength of the rock and when the rate of deformation is too fast to allow accommodation

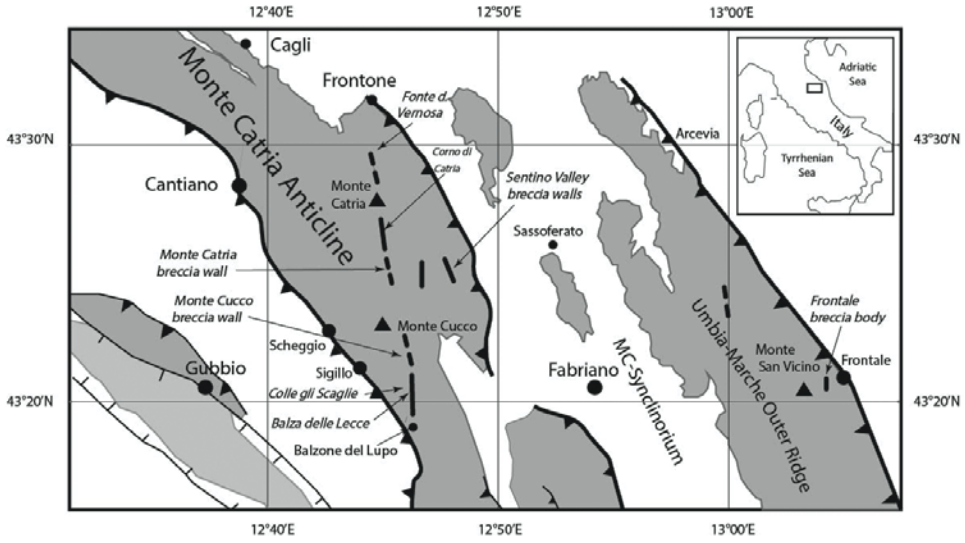

Figure 1. Occurrences of fluid-assisted breccia in the Umbria-Marche Apennines, based on maps in fig. 1 in Alvarez et al. (2019). MC—Matelica-Camerino.

of elastic strain through plasticity. An important point, critical to the discussion that follows, is that breccias do not form in the plastic domain, where high temperature or slow deformation rate enables the strain to occur by dislocation creep, grain boundary sliding, and grain rotation at a microscopic level without rupturing the rock at a mesoscopic scale. Volcanic and sedimentary breccias form through primary geological processes, and other major genetic types of breccia include collapse breccia, hydrothermal breccia, impact breccia, and explosion breccia. Fault breccias, as described in the Sibson-Scholz fault zone model (Sibson, 1977; Scholz, 1988; Imber et al., 2001), are commonly formed by kinematic processes. Since different subdisciplines of the geosciences may categorize breccias based on specific criteria and applications, classification schemes of breccias are sometimes complex and confusing (Ollier, 2007; Yang et al., 2017; Shukla and Sharma, 2018). In addition, a breccia that formed by one process can be altered in subsequent geological processes, and the brecciation and mineralization may not be cogenic with each other. For instance, the brecciation and mineralization of the solution-collapse breccia pipes in Arizona and that of the Wernecke breccia in Yukon probably occurred in separate geological events at different time periods (Wenrich, 1985; Laughton et al., 2005; Hunt et al., 2005, 2011).

Some classification schemes of breccia require a priori knowledge of the breccia's causal origin. Breccias that formed in hydrothermal conditions can be classified into phreatomagmatic, magmatic-phreatic, and phreatic breccias based on the components of magmatic volatiles and the origin of the hydrothermal fluids (Tămaș and Milési, 2002; Ollier, 2007). The distinctions among these breccias are based on whether the brecciation was incurred by direct encounter between water and magma, as well as the presence of magmatic volatiles in the hydrothermal fluid (see classification by Earth Science Australia at http://earthsci.org/mineral/rockmin/breccia/breccia.html). Jébrak (1997) proposed a comprehensive morphological classification of breccias based on the physical brecciation processes in hydrothermal vein-type deposits and stated that fluid-assisted hydraulic fracturing and critical fracturing, both caused by abrupt variations in fluid pressure, commonly produce in situ fragmentation of the host rocks and rapid precipitation of secondary minerals in the fractures. These classification schemes, however, are not readily applicable in the field description of breccia.

A morphological classification of breccia without specifying the genetic origin of the breccia and based upon the scheme devised by Sibson (1986) was proposed by Mort and Woodcock (2008) and Woodcock and Mort (2008). The scheme defines three types of breccia—crackle, mosaic, and chaotic breccia—based on the clast-infill ratio, with the roundness and amount of rotation of the clasts in the breccia used as additional qualifiers. The scheme also distinguishes among breccia, cataclasite, and "fault veins" on the basis of the size and percentage of clasts in the rock (Fig. 2). Clasts are defined to have a nominal diameter >2 mm, following the conventional definition of granules in the Wentworth Grain Size Scale. The infill may be a fine crushed matrix or cement. A kinematic rock comprising mostly crushed material of size <2 mm is considered a cataclasite. Fault veins

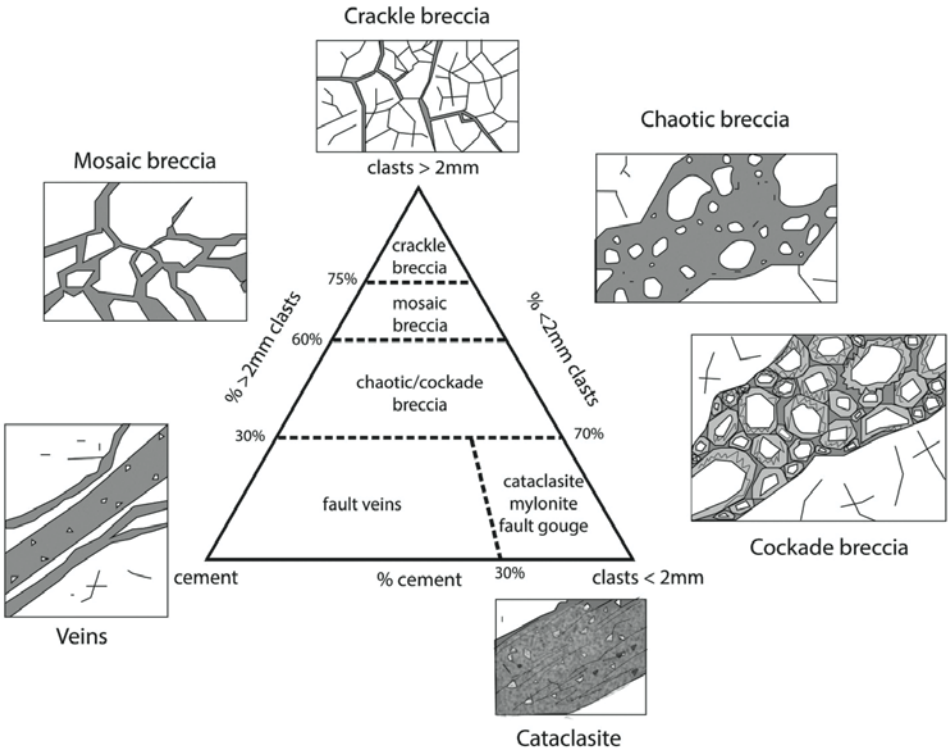

Figure 2. Ternary system for morphological classification of kinematic breccia and cataclasite (modified after Woodcock and Mort, 2008).

are basically mineral-filled fractures with less than 30% clasts, which often exhibit a preferred orientation but not any significant shear displacement. For crackle breccia and mosaic breccia that have >75% and 60%–75% clasts respectively, the clasts generally display no rotation and rounding, and adjacent fragments often would fit together. Chaotic breccia contains less than 60% clasts. Rotation and rounding of clasts are common in the chaotic breccia, indicating a certain extent of transportation of the clasts by the fluid.

Cockade breccia is a special kind of chaotic breccia containing clasts retained in a suspension state during the growth of secondary minerals. Breccias with cockade texture display overgrowths of secondary minerals, sometimes in concentric bands, forming a mantle around the clast fragments. The clast fragments are not in contact with each other, and the interstitial spaces among the banded mantle are filled by the same secondary mineral as the mantle overgrowths (Frenzel and Woodcock, 2014). Cockade breccia was reported to form in dilatational faults with fast-ascending fluids that kept the clasts in suspension (Cox and Munroe, 2016). The presence or absence of cockade texture may therefore reveal whether the brecciation occurred in a dilatational or compressional setting, and the distribution of various types of breccia within a brecciation zone can shed lights on the spatial variation of the hydrodynamical environment within the zone, as we will discuss below for the Colle gli Scoglie transect (location shown in Fig. 1).

NORTHERN APENNINES STRATIGRAPHY

An overview of the regional stratigraphy can provide geological context for discussion of fluid-assisted brecciation in the Maiolica limestone in the Umbria-Marche Apennines of Northern Italy. Such overviews are provided by Alvarez (1991), Centamore et al. (2002), Billi and Tiberti (2009), Molli et al. (2010), and Guerrera et al. (2012), among others. As described in the concise summary of Northern Apennines stratigraphy by Conti et al. (2020), an essentially continuous succession of platform-type sedimentary formations was deposited on the Umbria-Marche basement from Triassic to Paleogene time, spanning an interval of over 200 m.y. (Fig. 3). This generally conformable sedimentary sequence begins with the Upper Triassic Burano, a >2 km thick sequence of anhydrite, dolomites and marls formed in a lagoon-sabkha complex (Anelli et al., 1994, *as cited in* Conti et al., 2020).

During the first two stages of the Early Jurassic (Hettangian and Sinemurian), the region was a passive marine margin, with thick, shallow-water limestone beds several hundred meters in total thickness deposited on top of the Burano. The massive limestone known as the Calcare Massiccio is in turn overlain by a sequence of thinner-bedded sedimentary formations formed during a transition from shallow-water to pelagic conditions and representing the rest of the Jurassic. This transition was accompanied by extension and differential subsidence, causing the platform to break up into a series of small basins separated by tilted fault blocks whose crests formed a linear chain of seamounts (Santantonio and Carminati, 2011). The Jurassic sequence overlying the Calcare Massiccio is represented by a series of pelagic cherty limestones, marly limestones, micritic limestones, and calcarenites. The Complete Sequence, with a total thickness of a few hundred meters, was deposited in the basins, and the much thinner Condensed Sequence, comprising marl and limestone layers and called the Bugarone, was deposited on the seamounts.

The extensional faulting that affected the carbonate platform ended by about the beginning of Cretaceous time and was followed by deposition of the Maiolica, which is ~400 m thick in the basins and <100 m thick on seamounts. The Maiolica, the main focus of this chapter, consists predominantly of 10–50 cm thick beds of micritic limestone containing abundant black chert nodules. The limestone beds are separated from each other by thin black clay partings. The overlying Marne a Fucoidi is marked by a succession of black, green, and red marlstones with thin intercalations of limestones. The dark-colored and red marly layers were formed respectively during times of anoxic and oxygenated conditions (Giorgioni et al., 2017). The Marne a Fucoidi is in turn overlain by the Late Cretaceous–Paleogene pelagic limestones of the Scaglia sequence. It should be noted that the Umbria-Marche sedimentary sequence has recorded multiple events of synsedimentary deformation associated with extensional tectonics since the Jurassic (Baldanza et al., 1982; Decandia, 1982; Montanari et al., 1989; Tavarnelli and Peacock, 1999; Scisciani et al., 2001; Mirabella et al., 2004; Centamore et al., 2009; Tognaccini et al., 2019). Some of the synsedimentary faults controlling the thickness and facies differences within the Scaglia sequence also extend into the underlying Marne a Fucoidi and Maiolica (Tavarnelli, 1996).

It is important to highlight the roles played by the Burano and the Marne a Fucoidi in the process of brecciation in the Maiolica. The Calcare Massiccio overlying the Burano is, on a large scale, the most permeable formation in the area (Dragoni and Verdacchi, 1990; Cantucci et al., 2016). The post-Massiccio Jurassic sequence, with its alternations of limestone and marly formations, has relatively low permeability, while the Marne a Fucoidi behaves as an aquiclude above the Maiolica. The Calcare Massiccio and Maiolica therefore form the aquifers, while the Marne a Fucoidi forms a 50 m thick aquiclude, essentially isolating the Maiolica aquifer from the rocks above. The Calcare Massiccio–Upper Jurassic units–Maiolica-Marne a Fucoidi sequence represents an aquifer-aquitard-aquifer-aquiclude sequence as depicted in Figure 3. As discussed later in the Model of Maiolica Breccia Formation section, the Burano can readily deform in a plastic manner, which probably accounts for the source of the fluids responsible for the brecciation. The Marne a Fucoidi, on the other hand, forms the cap rock above the Maiolica, which facilitated the accumulation of over-pressured fluids in the Maiolica.

OCCURRENCES AND TIMING OF THE BRECCIA

The breccia reported by Alvarez et al. (2016, 2019) occurs primarily in the form of subvertical dike-like bodies in the

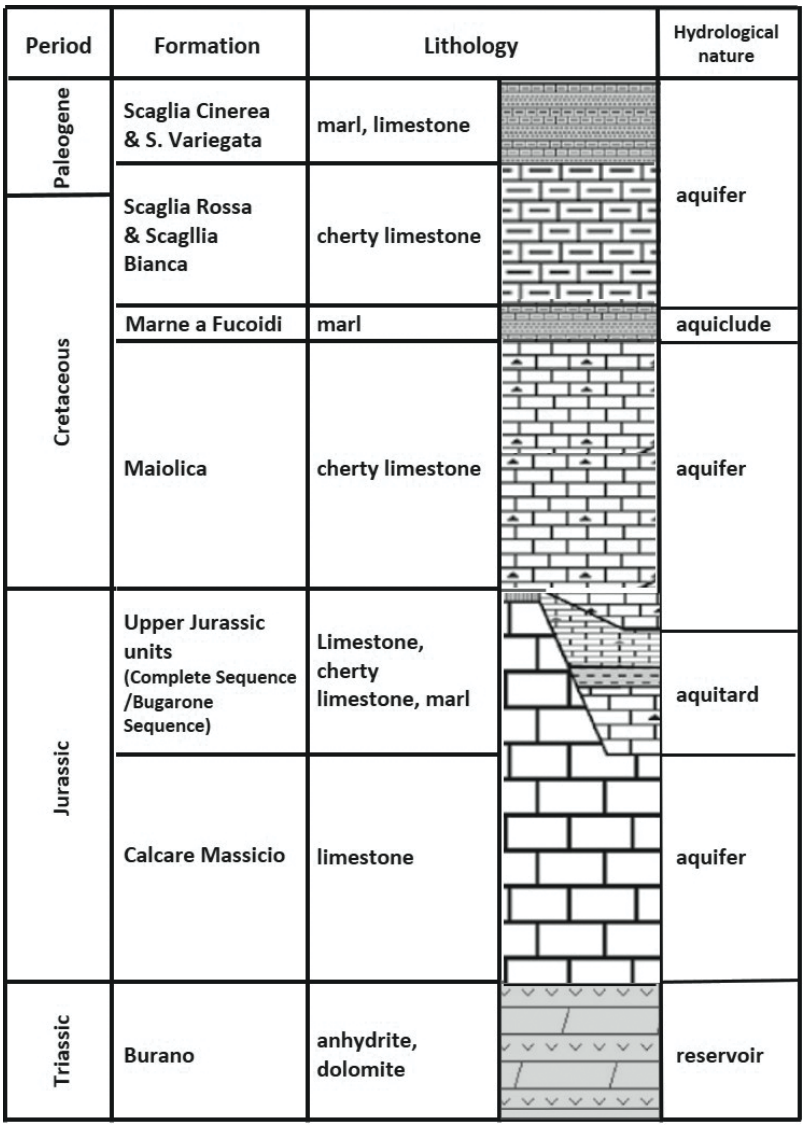

Figure 3. Triassic–Paleogene stratigraphy of the Umbria-Marche Apennines and hydrological nature of the main units.

Maiolica. In some places, the breccia dikes stand out as resistant white walls, referred to as "breccia walls" by Alvarez et al. (2019). The two largest breccia bodies form dike-like structures exposed intermittently on the crests of the Monte Catria and Monte Cucco anticlines (Fig. 1). The Monte Catria wall extends for 5.5 km from Fonte della Vernosa across the summit of Monte Catria and down the spur of the Corno di Catria, to the canyon of the Sentino River. The Monte Cucco wall extends for 2.5 km from the south slope of Monte Cucco to Balza delle Lecce near Sigillo. Two other occurrences of interest are at Balzone del Lupo near Sigillo and on the road from Frontale to Monte San Vicino (Alvarez et al., 2019). The Balza delle Lecce wall provides a unique 3D exposure of the breccia body that has not yet been studied in detail because of technical difficulties of access. In one place, the Monte Cucco wall is crossed by a rough service track along the south flank of the minor ridge of Colle gli Scoglie (43°21.514′N, 12°45.260′E, 1243 m elevation). Low road cuts along this track provide a unique transect extending for ~400 m across the breccia body; these exposures are described in Alvarez et al. (2019) and in the present chapter. The breccias at this locality generally comprise angular to subangular clasts ranging in diameter from a few mm up to 10 cm. The majority of the breccias observed are crackle and mosaic breccia, with chaotic breccias occurring in sporadic locations. Sometimes all three kinds of breccia can be found in the same exposure, showing that the hydrothermal flow regimes can vary greatly in different parts of the rock (Fig. 4).

The occurrences of the breccia walls along the crests of the anticlines suggest a causal relation between the brecciation and anticline development (although we cannot exclude the possibility that there may be breccias in synclines not exposed at the surface). Hydrothermal fluid injection producing the brecciation probably followed preexisting, fold-axis parallel extension faults. The lack of calcite twinning in the vein fills reported by Alvarez et al. (2019) has shed light on the depth for the occurrence of

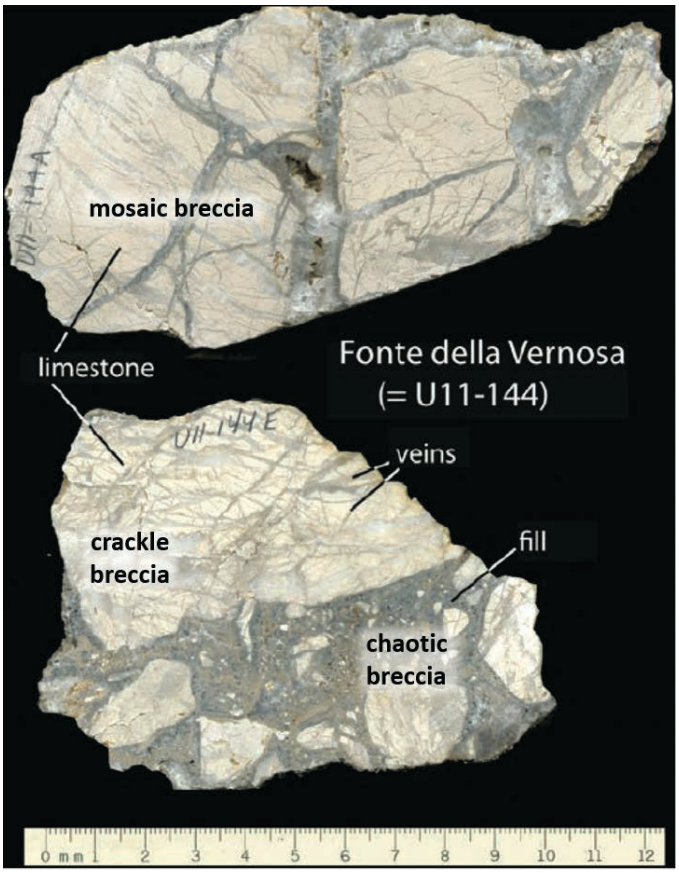

Figure 4. Rock slabs of a sample from Fonte della Vernosa near Monte Catria show the presence of three kinds of breccia in the same rock.

the brecciation. Groshong (1975) suggested a minimum deviatoric stress of 7 MPa for calcite twinning to form. Beaudoin et al. (2016) interpreted the experimental results obtained by Rowe and Rutter (1990) on calcite twinning as implying a minimum differential stress of 10 MPa for twining to occur. Since twinning structure was not observed in the vein calcite of the Maiolica, the brecciation probably occurred at a shallow depth at deviatoric stresses <7–10 MPa. The decrease in burial depth of the Maiolica was probably associated with the uplift and exhumation of the Northern Apennines. We may therefore suggest that the brecciation was a relatively late-stage event, occurring during Miocene or later tectonic deformation.

HYDRODYNAMIC IMPLICATIONS OF MAIOLICA BRECCIA

Flow Regimes of Hydrothermal Fluids

The flow regimes that occurred in various parts of the breccia body during its formation are manifested in the occurrence of different types of breccia along the Colle gli Scoglie track (Fig. 5; Alvarez et al., 2019, fig. 14). This transect is ~400 m long, with a well-exposed "solution tectonite" at chainage 105 m, dividing the breccia into an interior (eastern) and an exterior (western) section. This solution tectonite displays a distinctive S-C fabric and abundant presence of stylolites and marks the boundary between veined limestones and breccia (Alvarez et al., 2019). The limestones in the exterior section are not brecciated and show mineral-filled fractures and veins with preferred orientations, probably formed by mineral recrystallization in preexisting fractures. In the interior section, crackle breccia is pervasive, suggesting extensive crack development in the limestones incurred by the hydraulic fracturing. The interior section also consists of a 30 m wide core zone located at chainage 110–145 m and fringed by a marginal zone on each side. The core zone is marked by the presence of both mosaic and chaotic breccias, while the exposures in the fringe zones are characterized mainly by mosaic and crackle breccias.

The multiple types of breccia present in the same breccia body reveal spatially or temporally varying hydrodynamic regimes in the brecciation process. Peacock et al. (2019) suggested that extension in directions dictated by the preexisting faults implies a fluid pressure exceeding that of the least compressive stress, and when the breccia dike merges into a vein network, the fluid pressure was greater than that of the maximum compressive stress. The distribution of the various breccia types along the transect at Colle gli Scoglie reveals a gradient in the fluid regimes. As shown in the generalized model in Figure 6, the core zone of the interior section represents a high-flow regime zone dominated by chaotic and mosaic breccia. Individual veins of chaotic breccias display characteristics of fluidization and transport of the clasts. This high flow–regime zone is flanked by a low flow–regime zone dominated by crackle breccia on each side. In the expansion breccia, the fluid pressure is greater than the maximum principal stress and fractures developed in multiple directions oblivious to preexisting discontinuities in the rock. In the exterior section where mineral-filled fractures and veins instead of breccia are present, the fluid pressure was relatively smaller than that of the interior section but still greater than the minimum principal stress.

Tectonic Implications: Pumping vs Valving Events

In the conventional Coulomb failure model, fracturing occurs when the differential stress is greater than the shear strength of the rock. Such a critical condition can be produced either by increasing the maximum principal stress or by decreasing the minimal principal stress. The presence of preexisting fractures in a rock mass can reduce the elastic moduli and the tensile strength of the rock, and dictate the orientation of new ruptures. Cheng (2019) demonstrated a tendency for the dominant failure mode in rocks with preexisting fractures to change from shear failure to tensile failure. The injection of over-pressured fluids into existing fractures can increase the normal stress on the fracture walls. Continuous increase in the fluid pressure may cause at least one of the principal stresses to become tensional and produce a

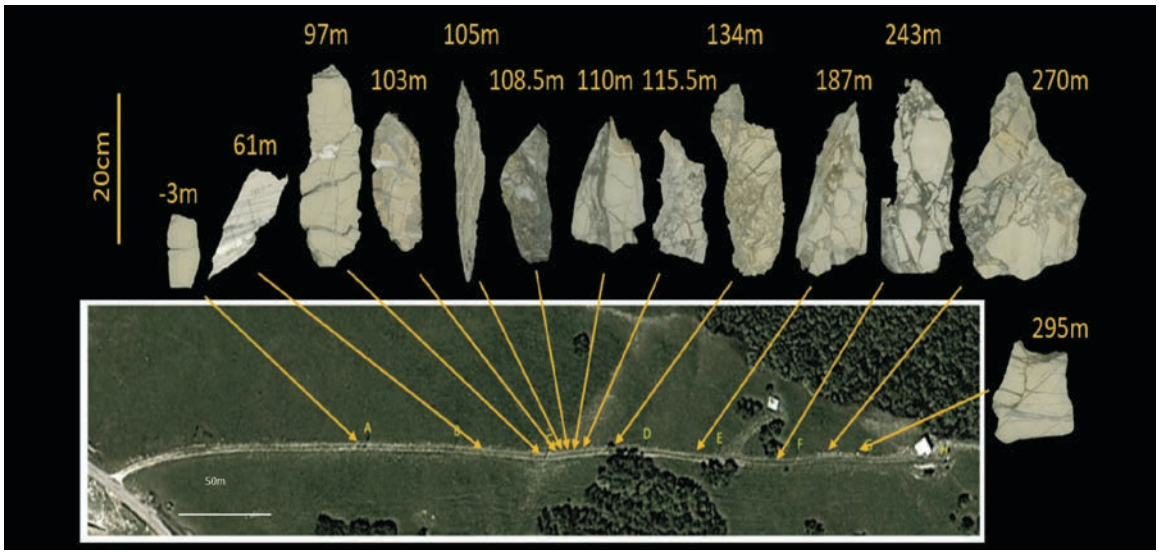

Figure 5. Interpretation of breccia types along the Colle gli Scoglie transect. The interpretation is superposed upon fig. 14 in Alvarez et al. (2019). The core zone of the interior section is located at chainage 110–140 m.

tensile stress sufficient to cause crack propagation at crack tips. On the other hand, a sudden increase in the porosity of the rock in a certain direction can decrease the confining pressure in that direction. In both cases, the differential stress can be modified to a level exceeding the tensile or shear strength of the rock, causing the rock to fail.

The hydrothermal fluids in fault zones may play one of two different roles in faulting events: seismic (fault) pumping or seismic (fault) valving (Sibson et al., 1975; Sibson, 1977, 1981). In seismic pumping, an earthquake plays an active role in the fracturing process. Fault movements associated with an earthquake produce a sudden increase in porosity and a reduction in fluid pressure, which in turn, result in implosive spalling of the wall rocks of the fault—a process referred to as critical fracturing by Jébrak (1997). Over-pressured fluids from below are then pumped into rupture-induced porosity along the fault. This kind of seismic or fault pumping is characteristic of a high-dilation tectonic environment, in particular where normal faulting or outer-arc stretching is taking place.

For the seismic (fault) valving process, the fault forms the closure and sealing mechanism against the fluid flow. Over-pressured hydrothermal fluid forces itself into existing fractures, leading to an increase in the differential stress and further fracturing or fault failures. The drop in the fluid pressure caused by the sudden fracturing allows the fault to collapse and close off the fluid conduit, and the fluid pressures to be maintained at a high level. Fault valving is often episodic in nature and occurs in a setting with a continuous supply of hydrothermal fluids.

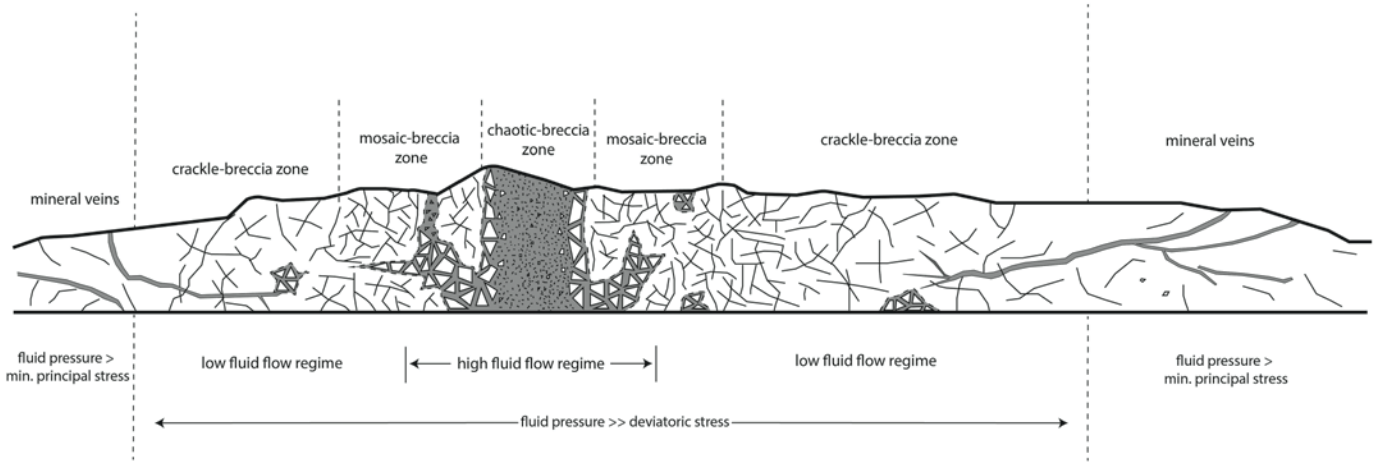

Figure 6. Generalized model of the Colle gli Scoglie transect showing breccia formed by different flow regimes. Min.—minimum.

We may determine from the morphological types of the Maiolica breccia whether the brecciation occurred by critical fracturing (fault pumping) or hydraulic fracturing (fault valving). Cockade breccia with mantle overgrowth around the clasts often provides insights into the fracturing state of a hydrothermal system, since it often forms from clast fluidization in rupture-controlled faults (Frenzel and Woodcock, 2014; Cox and Munroe, 2016; Berger and Herwegh, 2019). In this study, however, we have not seen any breccia with cockade texture in the Maiolica breccia. The absence of cockade breccia hence argues against significant fault dilation in the brecciation process, since the clasts were not suspended in the fluids long enough to allow mantle overgrowths to form around them. On the other hand, the pervasive presence of crackle breccia in the Maiolica breccia implies a condition of high fluid pressure sustained continuously in the brecciation process. We may infer from the field observations that the fluid-assisted brecciation in the Maiolica was achieved by an increase in fluid pressure (hydraulic fracturing) rather than an increase in porosity (critical fracturing), and that fault valving instead of fault pumping was the dominant process for the brecciation. This also implies steady injections of hydrothermal fluids to sustain over-hydrostatic pressures in the brecciation process.

Estimates of Fluid Velocity

The formation of the Maiolica breccia conceivably comprised two stages: (1) fragmentation of the wall rock by overpressured fluids, and (2) entrainment and transport of loosened clasts in the hydrothermal veins. Clast entrainment—the fluidization of aggregates of clasts—occurs when the drag force of the fluid flow overcomes the interparticle friction of the clasts. It is possible to determine analytically the fluid velocity from the grain size of the clasts and the hydrodynamical parameters of the fluid system, assuming the clasts behave as a cohesionless packed bed within the conduits of the fluid flow. Below a particular fluid flow rate referred to as the minimum fluidization velocity, the clasts remain densely packed and fluid flow occurs through the pore spaces in the rock. The gradual increase in the fluid velocity results in an increasing drag on the clasts and eventually causes the aggregates of clasts to become "fluidized."

The analytical solution for computing the minimum fluidization velocity is commonly based on the Ergun Equation (Ergun, 1952), which was first derived to estimate the pressure drop of fluid passing through a packed bed of particles (clasts) in a nuclear reactor. The Ergun Equation is given by

$$\Delta P = 150\,\frac{(1-\varepsilon)^2\mu v L}{\varepsilon^3\phi^2 D_P{}^2} + 1.75\,\frac{(1-\varepsilon)\rho_S v^2 L}{\varepsilon^3\phi D_P}, \quad (1)$$

in which ΔP is the pressure drop as the fluid passes through the packed bed of clasts, ε is the voidage (porosity), v is the fluid velocity, μ is the fluid viscosity, L is the length of the channel, ϕ is the clast sphericity, and D_P is the clast diameter. The two terms in Equation 1 correspond to the contributions from the laminar and turbulent flow, respectively.

The balance between the weight of the clasts in the fluid and the upward force exerted on the clasts can be expressed by

$$\Delta P = (1-\varepsilon)(\rho_S - \rho_f)Lg, \quad (2)$$

in which ρ_S and ρ_f are the density of the solid and fluid, respectively, and g is gravitational acceleration. Many experiments in chemical engineering have demonstrated the efficacy of the Ergun Equation to predict the fluidization velocity for various clast size and flow regimes. The Ergun Equation has also been modified into various forms to account for variations in clast size and shape, and geometry of the fluid channel. A detailed review of the empirical coefficients used in the Ergun Equation is given by Quinn (2014).

For geological applications, the Ergun Equation or its modified forms are used in diverse situations to study the velocity needed for sediment motions, pyroclastic current flow, liquefaction of slope material, and fluidization of fault gouge, etc. (Allen, 1982; Cheng, 2003; Valverde, 2015; Breard et al., 2019). In particular, the two equations above are often modified for the computation of v, the fluid velocity needed to stimulate clast entrainment in a fluid system. For a channel flow with relatively large clast size, turbulent flow dominates and the first term in the Equation can be ignored, leading to a simplified expression that can be used to estimate the fluidization velocity in a channel of packed clasts, i.e.,

$$v = \sqrt{\left(\frac{\phi D_P(\rho_S-\rho_f)g\varepsilon^3}{1.75\rho_f}\right)}. \quad (3)$$

The sphericity ϕ is dependent on the clast geometry and varies mostly between 1.0 and 2.5 for natural sediment (Gidaspow, 1994; Zheng and Hryciw, 2015). Since most of the other parameters in Equation 3 can be derived readily, the minimal fluidization velocity can be estimated from clast size. Berger and Herwegh (2019) estimated the velocity needed for suspension of clasts of 2.5 mm size to be ~0.11 m/s in a cockade breccia. Oliver et al. (2006) applied Equation 3 above to obtain a velocity of ~20 m/s for fluidizing breccia clasts in the Cloncurry Fault of Australia.

The minimum fluidization velocity is found to be sensitively related to the size of the clasts as well as the porosity of the packed clasts. Figure 7 shows the computed fluidization velocity plotted against clast size at submeter range for initial porosity values of 0.2, 0.5 and 0.7, assuming a value of 1.0 for sphericity, and 2600 kg/m^3 and 1000 kg/m^3 for bulk density of the clasts and the fluid, respectively. The porosity values are found to affect the minimum fluidization velocity by a factor of 2–5 (Fig. 7). Also, the fluidization velocity needed for clast entrainment is smaller for a bed with lower porosity, since a low-porosity bed results in a greater pressure drop by the same fluid velocity.

The velocity required to sustain entrained clasts in the fluid flow, however, differs from the minimal fluidization velocity

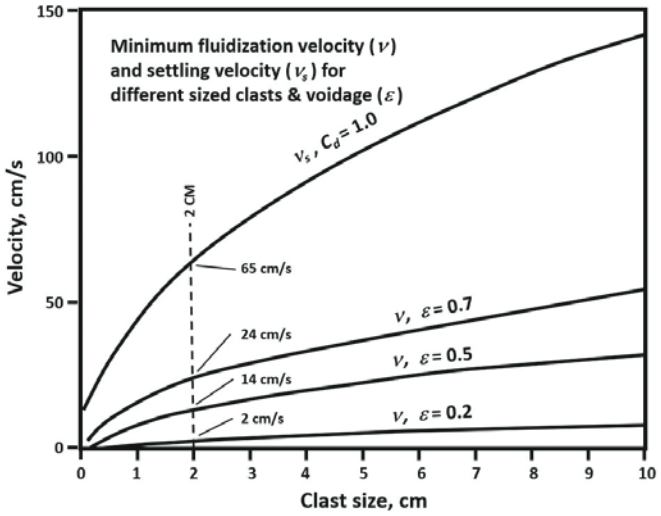

Figure 7. Minimum fluidization velocity and settling velocity for various sized clasts plotted for porosity of 0.2, 0.5 and 0.7 and drag coefficient Cd = 1.0.

needed for the clast entrainment. Once the aggregate of clasts is fluidized, the porosity of the bed increases, and a greater velocity is needed to sustain the clasts in the fluid. The fluid velocity needed for keeping the clasts in suspension can be estimated from the settling velocity of the clasts, which is about an order of magnitude greater than the fluidization velocity (Allen, 1982). The settling velocity, ν_S, depends on the particle diameter D_p as well as the drag coefficient, C_d, a dimensionless parameter governed by the flow regime and particle geometry (Gabitto and Tsouris, 2008):

$$\nu_s = \sqrt{\left(\frac{4(\rho_S - \rho_f)gD_P}{3C_d}\right)}. \quad (4)$$

Many studies show that the values of C_d range between 0.5 and 2, with cylindrical clasts approaching a value of 1.0 for intermediate to turbulent flow conditions. For a C_d of 1.0, the settling velocity obtained is found to be greater than the fluidization velocity by approximately a factor of 5 in the present study. While the velocity needed is obviously far smaller in horizontal conduits, the settling velocity yields the minimum velocity to transport the clasts in vertical conduits.

The largest clasts involved in the fluidized flow can be used as an indication of the minimum fluid velocity achieved in the hydrothermal system. As shown in Figure 5 (redrawn from fig. 14 in Alvarez et al., 2019), the samples along the section in Colle gli Scoglie comprise several kinds of breccia with different clast sizes. The breccias with very large clasts are simply fractured into crackle breccias. Mosaic breccias are observed to contain clasts with a nominal diameter of 3–4 cm. The largest clasts in the chaotic breccia that are found to be rounded are ~2 cm in diameter. As shown in Figure 7, using 2 cm for D_p and porosity values of 0.2, 0.5 and 0.7, the estimated minimum fluid velocities for the clast entrainment are in the range of 2–24 cm/s, and a velocity of ~65 cm/s (~2.3 km/h) was obtained for sustaining the clast in suspension in vertical veins.

Fragmentation Mechanisms

The analysis given in the "Estimates of Fluid Velocity" section yields estimated velocities for entrainment and suspension of clasts, assuming the clasts form a packed bed with no cohesion or internal strength. A separate mechanism, however, is needed for fragmentation of limestone into broken clasts in the first place. Fragmentation can occur when the external stress exceeds the tensile strength of the rock. As discussed in the Occurrences and Timing of the Breccia section, the deviatoric stress of the Maiolica breccia was less than 7–10 MPa, based on the presence of stylolites and the absence of twinning in the calcite matrix, essentially confining the brecciation to occur within 500 m of the surface. The deviatoric stress at such a shallow depth is unlikely large enough to rupture the limestone directly. The fragmentation was probably achieved by fluid-assisted crack formation and crack-tip propagation.

Preexisting discontinuities in the rock, including faults, joints, cleavages, stylolites, and micro-fissures, are all vulnerable to the crack growth process. Analytical studies of fault mechanics generally point to the existence of very large deviatoric stresses at fault tips, which can overcome the tensile strength of the rock readily. At the tips, crack growth can be achieved by pulling apart the fracture planes (Patrício and Mattheij, 2007). Hence, the preexistence of cracks in rocks can enable crack growth at stresses lower than that required for slip or twinning. For the case of the Maiolica breccia, the over-pressured fluid probably produced a widening and infilling of the fractures, leading to formation of crackle and mosaic breccias. The limestone continued to fracture until some of the clasts broke away from the host rock and became completely bounded by veins.

As shown by Abé et al. (1976), a constantly high fluid pressure is needed to sustain the crack growth process, which also requires rapid closure of any newly formed fractures to sustain the high fluid pressure. A sudden decrease in the partial pressure of CO_2 associated with newly formed fractures could, in turn, facilitate rapid precipitation of calcite in newly formed veins. The presence of dissolved silica may play a role in expediting the carbonate precipitation as well as the polymorphic species of the carbonate. The carbonate precipitated in a low-temperature "pure" system without silica is likely vaterite and aragonite. Over time, vaterite would convert to the more stable phase of calcite. The experimental work by Kellermeier et al. (2013) shows that silica can increase the growth rate of calcite and inhibit the formation of the other polymorphs. High fluid temperatures may also lead to rapid calcite growth with the presence of dissolved silica (Lakshtanov and Stipp, 2010). In all cases, the rapid formation of calcite cement in the cracks probably inhibited fluid flow and enabled high fluid pressure to be sustained during the brecciation of the Maiolica.

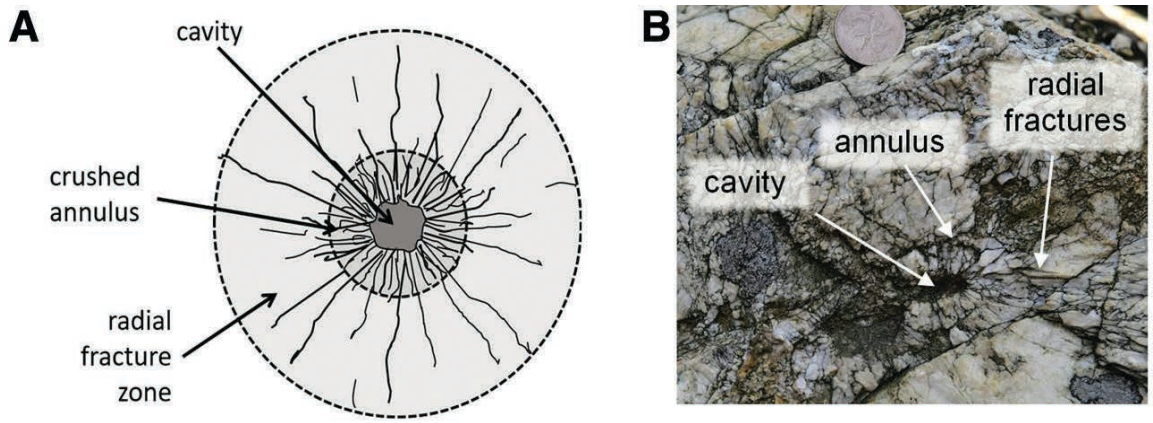

Figure 8. (A) Generalized pattern of explosion fractures showing a central cavity, a crushed annulus, and a zone of radial fractures. (B) Example of an explosion fracturing pattern in a quartz dike in Hong Kong.

Explosion Fractures

The fracturing pattern in the breccia may bear information on the stress configuration during the brecciation process. In cases where new veins or fractures are formed by expansion of preexisting cracks, the orientation of the veins or fractures is governed by the orientation of the cracks, and in cases where tensile fracturing of intact rock takes place, fracture orientation is controlled by the configuration of the stress field. In the mosaic breccias of the Maiolica, some vein and fracture patterns are found to resemble the pattern formed during explosions accompanying quarry blasts. In quarry blasts, the conversion of chemical energy into gaseous expansion can produce a shock wave with a pressure in the range of 0.5–50 GPa, readily overcoming the tensile strength of near-surface rocks (Saharan et al. 2006). As shown in the example in Figure 8, an explosion fracturing pattern generally comprises a cavity in the epicenter, a crushed annulus with dense fractures and an exterior zone with radial cracks (Loorents et al., 2000; Mitelman and Elmo, 2014; Saharan et al. 2006).

Figure 9 shows a fracturing pattern in the Maiolica limestone exposed in the Frontale locality that closely resembles an explosion fracturing pattern. In this exposure, crackle breccia and mosaic breccia with relatively larger clasts are present around several chaotic breccia veins. The clasts in the chaotic breccias are relatively more rounded and smaller in size. On the right side of the picture, some fractures are found to radiate from a nucleus. The cavity was filled by sparry calcite and clasts. The fracture pattern is not exactly radial, as in the example in Figure 8B, since the fractures were apparently affected by preexisting discontinuities in the limestone. Alvarez et al. (2016) pointed out that the conversion from liquid to gas in the carbonate could produce a substantial volumetric change and pressure. The explosive rupturing could be caused by sudden reduction of the fluid pressure, causing the superheated fluid to reach the water saturation

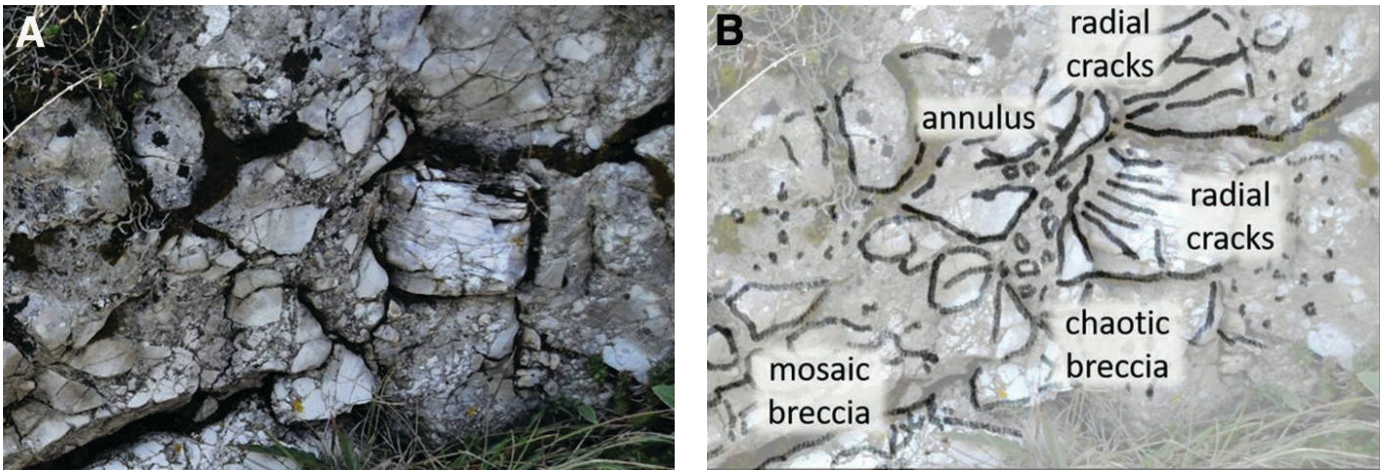

Figure 9. (A) Suspicious explosion fractures in Maiolica limestone near Frontale. (B) The interpretative diagram showing the annulus, which is filled by matrix and cement, and radial crack zone.

line and producing a boiling liquid expanding vapor explosion (BLEVE) similar to the explosion of a fractured gas tank.

We may assume that the liquid-gas transformation occurs below the supercritical temperature of water of 374 °C, since above that temperature, water and steam are indistinguishable from each other. Assuming a temperature of 200 °C, liquid boiling occurs at ~1.55 MPa. At that liquid-vapor boundary, the specific volume is 0.0012 m^3/kg and 0.1276 m^3/kg, respectively, for saturated water and steam, yielding an expansion ratio of ~110. The space confinement in the fractures necessarily results in a sudden increase in pressure by 110×, fracturing the rocks in the vicinity of the vaporization center and producing a rupture pattern that is unaffected by the local deviatoric stress state.

The presence of explosion fracture patterns in an exposure is conducive to the determination of the P-T path of the over-pressured hydrothermal fluids. Vaporization occurs when the over-pressured fluids reach the water saturation line in the phase diagram of water. Suppose the water fluids originate at a depth of ~5 km with an initial temperature of 200 °C and at a pressure of 130 MPa. The fluids may follow one of the three P-T paths in their ascent to the earth's surface. For path A in Figure 10, the fluids ascend very quickly through fractures and pores to reach the saturation line, maintaining a steady temperature at close to 200 °C. The vaporization is essentially incurred by the reduction in the pressure. In this case, we may expect intensive occurrence of fractures due to expanding vapor explosion. For Path B, the over-pressured fluids lose heat by conduction and convection while ascending through the brittle zone and reach the saturation line at a lower temperature and pressure. Explosion fracturing still occurs but likely at a relatively lower intensity compared to that of Path A. For Path C, the over-pressured fluids ascend through the brittle zone with a velocity sufficiently slow to enable much heat loss during the ascent. The fluids are maintained in a liquid state and likely emerge on the surface as high-temperature spring water without vaporization. No explosion fractures are expected to be present in the rock in such a scenario.

Explosion-fracturing structures are not commonly present in the Maiolica breccia. The example shown in Figure 9 plausibly resulted from explosion fracturing and can only be regarded as a suspicious case. We may infer that the over-pressured fluids producing the brecciation in the Maiolica limestone probably followed a P-T path similar to Path C in Figure 10. Only in isolated vents or fractures may the fluids have reached the saturation line to produce explosion fracturing, while the majority of the brecciation occurred with the hydrothermal fluids never reaching the water saturation line, and therefore emerging onto the surface as spring water.

MODEL OF MAIOLICA BRECCIA FORMATION

A key question pertaining to the fluid-assisted formation of the Maiolica breccia is the origin of the hydrothermal fluids for hydraulic fracturing. Recent studies showed that expulsion of fluids from the plastic zone by sudden increases in porosity and permeability can form channelized fluid flows at velocities much greater than the background flow rate determined by Darcy's Law (Connolly and Podladchikov, 2015; Chakraborty, 2017; Jordan et al., 2018). The rapid fluid flow is also found to be associated with high fluid pressure close to lithostatic pressure. Peacock et al. (2019) showed that when the fluids in two rock masses with markedly different fluid pressure connect suddenly to form a single fluid column, fluid-assisted brecciation can occur in the higher rock mass. Geological processes such as earthquakes, magmatism, and devolatilization during regional

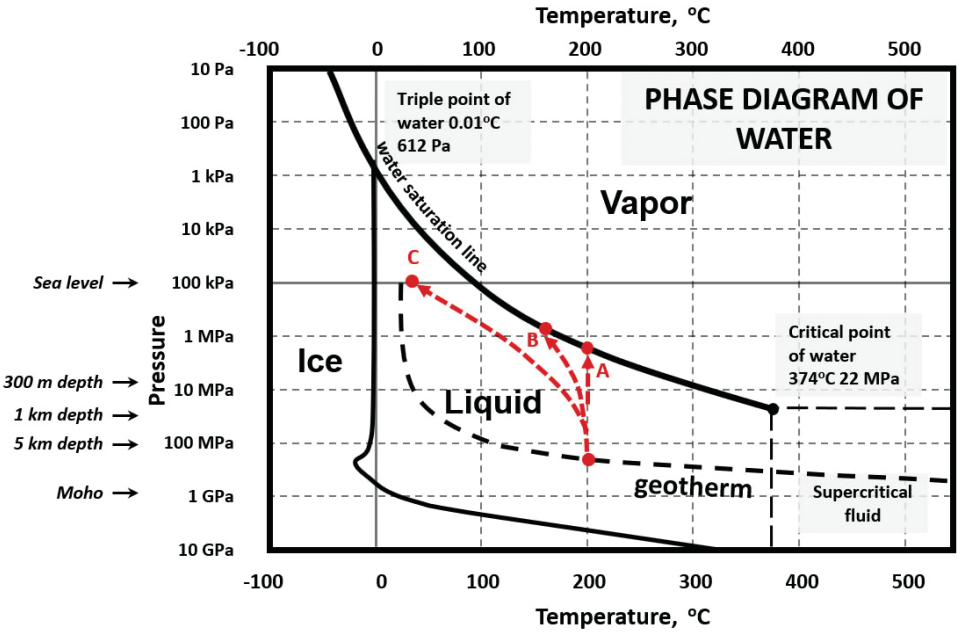

Figure 10. Possible P-T paths of over-pressured water plotted on the phase diagram of water. For Paths A and B, water-steam transformation occurs when the fluids reach the water saturation line. For Path C, the over-pressured fluids lose heat rapidly and allow the fluids to remain in a liquid state before reaching Earth's surface.

metamorphism may also produce fluid flow (Connolly, 1997). Fournier (1999) presented a model on the formation of hydrothermal breccia associated with extensive silicification and mineralization by breaching water seals in the plastic zone. In the model, the depth of the brittle-plastic (B-P) transition around a magmatic body depends on material, temperature, creep rate, and stress configuration. Progressive cooling of the magmatic body can result in a deepening of the B-P boundary, causing crustal material to migrate from the plastic domain to the brittle domain and liberation of over-pressured fluids from the B-P transition zone. Such a fluid injection process would probably produce hydraulic fracturing rather than pore inflation (Bailey, 1990).

There are no known magmatic events in the Umbria-Marches region that could have led to deepening of the B-P boundary by crustal cooling. However, the deepening could be accomplished by unroofing, either by erosion of the cover or tectonically by large-scale normal faulting, which has been an important feature in the very young history of the Umbria-Marche Apennines. The crustal B-P boundary is generally located at crustal depths of 10–15 km (Sibson 1977). Kusznir and Park (1986) and Scuderi et al. (2015) show that multiple or localized B-P transitions can exist in the crust. For the Umbria-Marches region, the Triassic Burano could achieve plasticity at fairly shallow depth. The study by Chester (1988) shows that halite can deform by dislocation creep at normal stress below 50 MPa, causing halite to behave in a plastic manner at very shallow depths. The fluid inclusion study by Lugli (2001) also reveals a paleotemperature of ~300 °C experienced by the Burano. At that temperature and depth, Burano would behave as a plastic material. For that reason, the brittle-plastic transition for the Burano may conceivably be present at a relatively shallow depth compared with that in crystalline rocks. Santantonio and Carminati (2011) show the termination of the faults forming the seamounts and basins at the Burano, hence implying a plastic state of the Burano during the Early Jurassic. Lugli (2001) also showed that Burano experienced a deepening during the Oligocene, attaining a burial depth of over 10 km, followed by shallowing to ~500 m during late- to post-Miocene time. Such depth changes may have caused the Burano to follow a brittle-plastic-brittle path in its geological history.

The high plasticity of the Burano would cause the rock to deform by plastic flow, resulting in very low permeability (Fig. 11A). Brine solutions trapped in sealed cavities or lenses of high-porosity dolostones surrounded by evaporite inside the Burano were under lithostatic pressure at a gradient of ~27 MPa/km. The migration of the Burano into the brittle field during the exhumation of the Northern Apennines would have caused a sudden increase in permeability and breaching of the water pockets (Fig. 11B). A sudden connection with fractures in the brittle zone can expose the water to the hydrostatic pressure, resulting in over-pressured fluids being injected into the fracture systems. If the water is in a supercritical state, the water can penetrate fractures readily since supercritical water has no surface tension. Supercritical water also has relatively greater dissolving ability. The reversal from a supercritical to a liquid state can result in extensive precipitation of the dissolved material.

The high-pressure hydrothermal brines liberated from the Burano would quickly ascend through the Calcare Massiccio and the Maiolica (Fig. 11B). The Marne a Fucoidi, as an aquiclude, rendered further upward migration of the fluids difficult and resulted in accumulation of over-pressured fluids in the Maiolica, causing hydraulic fracturing in the limestone. The Calcare Massiccio was not brecciated because of the presence of faults and conduits that allowed through-flow of the hydrothermal brine. It is also generally thick-bedded, making it relatively more difficult to fracture hydraulically on a large scale. Ladeira and Price (1981) and Petrie et al. (2012), among others, demonstrate such an inverse relation between fracture density and bed thickness. The Maiolica, being relatively thin-bedded, was readily fractured, accounting for the presence of extensive brecciation. The Scaglia sequence above the Marne a Fucoidi was affected when the fluids found their way into the Scaglia sequence. Locally, the hydrothermal brines might follow preexisting faults in the Marne e Fucoidi, forming subvertical breccia zones extending into the Scaglia (Fig. 11B), as exemplified by the breccia wall at Balzone del Lupo near Sigillo.

CONCLUSION

This study proposes Neogene exhumation of the Apennines that brought the Burano evaporites up from a depth below the B-P transition to a depth above the B-P transition as the cause of fluid-assisted brecciation in the Maiolica Limestone. The fluctuation of the B-P transition, which could be a transient or a permanent phenomenon, can have significant implications for a wide range of geological processes. Earthquake-induced transient increase in the depth of the B-P boundary was reported by Cheng and Ben-Zion (2019) and Zielke et al. (2018). In such an incident, the extension of fault-slip into the plastic domain may cause a temporary deepening of the B-P transition. Subsequent deformation may gradually revert the rocks back to a plastic state. The deepening of the B-P zone caused by crustal exhumation is probably a more permanent one. The model can be used to explain the occurrences of hydrothermal mineralization in amagmatic regions. Chan (2019) attributed the extensive hot spring activities in Guangdong Province in China to a similar deepening of the B-P transition. The concept offers a plausible explanation for hot springs observed in many nonvolcanic regions of the world.

This chapter complements earlier reports by Alvarez et al. (2016, 2019) and Belza et al. (2019) on the field description and geochemical study of the Maiolica breccia with an analysis of the hydrodynamical implications of the brecciation process. The key inferences in this chapter are as follow.

1. Different flow regimes are recorded in the breccia transect of Colle gli Scoglie, with crackle breccia pervading the limestone, and mosaic and chaotic breccias characterizing a high-flow regime in the core zone of the transect. Mineral-filled fractures and veins occurred in the marginal zones of the breccia body.

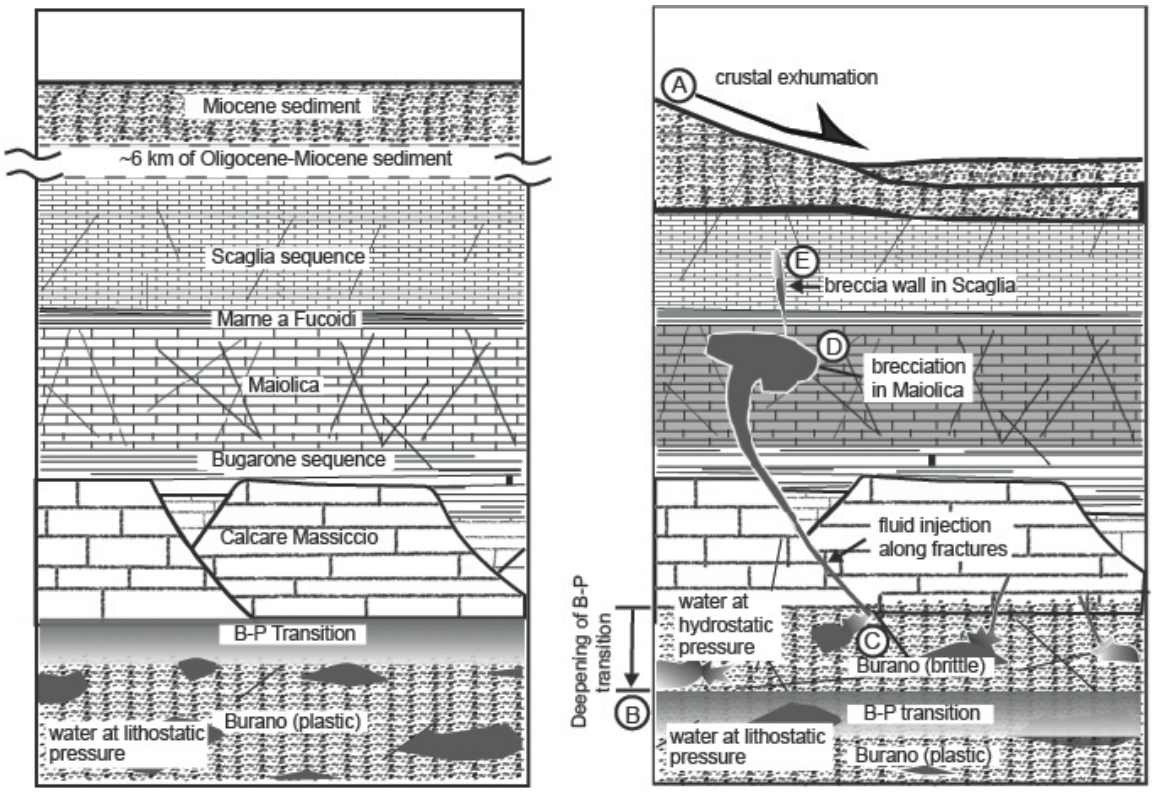

Figure 11. Model of formation of the Maiolica breccia. (A) Pre-exhumation situation with brittle-plastic (B-P) transition located approximately at the top of the Burano formation. The deep burial depth kept the Burano in a plastic state, and the low permeability caused water to be encapsulated in isolated pockets. (B) Deepening of the B-P transition resulting from crustal exhumation (A) caused the Burano to migrate into the brittle domain (B), which led to breaching of water seals (C) and fluid injection of brine solution into the overlying limestones. Fluid pressure accumulated at the top of the Maiolica with the Marne a Fucoidi acting as an impermeable cap rock, producing the brecciation (D). Some over-pressured fluids ascended through the Marne a Fucoidi along faults to form breccia dikes in the overlying Scaglia sequence (E).

2. The lack of cockade-texture breccia implies sustainment of high hydraulic pressures in the fractures. Fault-valving rather than pumping was likely the dominant seismic state associated with the brecciation.

3. Based on the breccia morphology and clast sizes, the fluid velocity attained was ~2–24 cm/s for fluidization of the clasts and ~65 cm/s (~2.3 km/h) for sustaining the clasts in motion.

4. Explosion fracturing patterns formed by expanding vapor explosion at shallow crustal depths are not common in the Maiolica breccia. The bulk of the hydrothermal fluids probably found its way onto Earth's surface without vaporization in the subsurface.

5. The Burano anhydrite probably constitutes the source of the hydrothermal fluids.

6. The fluid-assisted brecciation was probably associated with exhumation of the Umbria-Marche Apennines, which caused a deepening of the B-P transition and breaching of water seals in the plastic zones, especially in the Burano anhydrite.

7. The rheological transition from plastic to brittle domain experienced by the Burano during the late Miocene could have resulted in liberation of trapped brines at lithostatic conditions and the hydraulic injection events.

8. The contrast in permeability between Marne a Fucoidi and Maiolica resulted in the accumulation of over-pressured fluids in the Maiolica and brecciation of the limestone.

9. Where an existing fault cut through the Marne a Fucoidi, over-pressured fluids ascended into the Scaglia sequence, forming breccia dikes in the Scaglia.

While some of the interferences above are necessarily speculative, this study highlights the possibility of integrating cross-disciplinary findings and field observations in reconstruction of geological models, and points to topics for further research and analyses.

ACKNOWLEDGMENTS

The authors are indebted to Stephen Marshak and Philippe Claeys for thorough reviews of the manuscript. Research support for Chan from ProjecTerrae in Hong Kong is gratefully acknowledged.

REFERENCES CITED

Abé, H., Mura, T., and Keer, I.M., 1976, Growth rate of a penny-shaped crack in hydraulic fracturing of rocks: Journal of Geophysical Research, v. 81, no. 29, p. 5335–5340, https://doi.org/10.1029/JB081i029p05335.

Allen, J.R.L., 1982, Liquidization, liquidized sediment, and the sedimentation of dense particle dispersions, *in* Allen J.R.L., ed., Sedimentary Structures: Their Character and Physical Basis: Amsterdam, Elsevier, Developments in Sedimentology, v. 30, Part B, p. 293–342.

Alvarez, W., 1991, Tectonic evolution of the Corsica-Apennines-Alps region studied by the method of successive approximations: Tectonics, v. 10, no. 5, p. 936–947, https://doi.org/10.1029/91TC00232.

Alvarez, W., Belza, J., Peacock, D., Claeys, P., and Tavarnelli, E., 2016, Expansion breccias in carbonate rocks: Geological Society of America Abstracts with Programs, v. 48, no. 7, https://doi.org/10.1130/abs/2016AM-282404.

Alvarez, W., Belza, J., Chan, L.S., Claeys, P., Geiser, P., Menichetti, M., Shimabukuro, D.H., and Tavarnelli, E., 2019, Expansion breccias in Lower Cretaceous Apennine pelagic limestones: I. Geological observations, *in* Koeberl, C., and Bice, D.M., eds., 250 Million Years of Earth History in Central Italy: Celebrating 25 Years of the Geological Observatory of Coldigioco: Geological Society of America Special Paper 542, p. 229–250, https://doi.org/10.1130/2019.2542(12).

Bailey, R.C., 1990, Trapping of aqueous fluids in the deep crust: Geophysical Research Letters, v. 17, no. 8, p. 1129–1132, https://doi.org/10.1029/GL017i008p01129.

Baldanza, A., Colacicchi, R., and Parisi, G., 1982, Controllo tettonico sulla deposizione dei livelli detritici nella Scaglia Cretaceo-Paleocenica (Umbria Orientale): Rendiconti della Società Geologica Italiana, v. 5, p. 11–14.

Beaudoin, N., Koehn, D., Lacombe, O., Lecouty, A., Billi, A., Aharonov, E., and Parlangeau, C., 2016, Fingerprinting stress: Stylolite and calcite twinning paleopiezometry revealing the complexity of progressive stress patterns during folding—The case of the Monte Nero anticline in the Apennines, Italy: Tectonics, v. 35, 1687–1712, https://doi.org/10.1002/2016TC004128.

Belza, J., Alvarez, W., Tavarnelli, E., Vanhaecke, F., Baele, J.-M., and Claeys, P., 2019, Expansion breccias in Lower Cretaceous Apennine pelagic limestones: II. Geochemical constraints on their origin, *in* Koeberl, C., and Bice, D.M., eds., 250 Million Years of Earth History in Central Italy: Celebrating 25 Years of the Geological Observatory of Coldigioco: Geological Society of America Special Paper 542, p. 251–269, https://doi.org/10.1130/2019.2542(13).

Berger, A., and Herwegh, M., 2019, Cockade structures as a paleo-earthquake proxy in upper crustal hydrothermal systems: Scientific Reports, v. 9, p. 9209, https://doi.org/10.1038/s41598-019-45488-2.

Billi, A., and Tiberti, M.M., 2009, Possible causes of arc development in the Apennines, central Italy: GSA Bulletin, v. 121, no. 9/10, p. 1409–1420, https://doi.org/10.1130/B26335.1.

Breard, E.C.P., Jones, J.R., Fullard, L., Lube, G., Davies, C., and Dufek, J., 2019, The permeability of volcanic mixtures—Implications for pyroclastic currents: Journal of Geophysical Research: Solid Earth, v. 124, no. 2, p. 1343–1360, https://doi.org/10.1029/2018JB016544.

Cantucci, B., Montegrossi, G., Lucci, F., and Quattrocchi, F., 2016, Reconstruction of rocks petrophysical properties as input data for reservoir modeling: Geochemistry Geophysics Geosystems, v. 17, p. 4534–4552, https://doi.org/10.1002/2016GC006548.

Centamore, E., Fumanti, F., and Nisio, S., 2002, The Central-Northern Apennines geological evolution from Triassic to Neogene time: Bollettino della Società Geologica Italiana, Volume speciale no. 1, p. 181–197.

Centamore, E., Rossi, D., and Tavarnelli, E., 2009, Geometry and kinematics of Triassic-to-Recent structures in the Northern-Central Apennines: a review and an original working hypothesis: Italian Journal of Geosciences, v. 128, p. 419–432, https://doi.org/10.3301/IJG.2009.128.2.419.

Chakraborty, S., 2017, A new mechanism for upper crustal fluid flow driven by solitary porosity waves in rigid reactive media?: Geophysical Research Letters, v. 44, no. 20, p. 10324–10327, https://doi.org/10.1002/2017GL075798.

Chan, L.S., 2019, A model for the formation of hot springs in coastal area of Guangdong: Conference Proceedings, The 9th World Chinese Conference of Geological Science, Jilin, China, 1–2 June, Session 1, p. 9.

Cheng, N.S., 2003, Application of Ergun equation to computation of critical shear velocity subject to seepage: Journal of Irrigation and Drainage Engineering, v. 129, no. 4, p. 278–283, https://doi.org/10.1061/(ASCE)0733-9437(2003)129:4(278).

Cheng, X., 2019, Damage and failure characteristics of rock similar materials with pre-existing cracks: International Journal of Coal Science and Technology, v. 6, no. 4, p. 505–517, https://doi.org/10.1007/s40789-019-0263-4.

Cheng, Y., and Ben-Zion, Y., 2019, Transient brittle-ductile transition depth induced by moderate-large earthquakes in Southern and Baja California: Geophysical Research Letters, v. 46, n. 20, p. 11109–11117.

Chester, F.M., 1988, The brittle-ductile transition in a deformation-mechanism map for halite: Tectonophysics, v. 154, p. 125–136.

Clark, C., and James, P., 2003, Hydrothermal brecciation due to fluid pressure fluctuations: examples from the Olary Domain, South Australia: Tectonophysics, v. 366, no. 3–4, p. 187–206, https://doi.org/10.1016/S0040-1951(03)00095-7.

Connolly, J.A.D., 1997, Devolatilization-generated fluid pressure and deformation-propagated fluid flow during prograde regional metamorphism: Journal of Geophysical Research, v. 102, p. 18149–18173, https://doi.org/10.1029/97JB00731.

Connolly, J.A.D., and Podladchikov, Y.Y., 2015, An analytical solution for solitary porosity waves: Dynamic permeability and fluidization of nonlinear viscous and viscoplastic rock: Geofluids, v. 15, p. 269–292, https://doi.org/10.1111/gfl.12110.

Conti, P., Cornamusini, G., and Carmignani, L., 2020, An outline of the geology of the Northern Apennines (Italy), with geological map at 1:250,000 scale: Italian Journal of Geosciences, v. 139, p. 149–194, https://doi.org/10.3301/IJG.2019.25.

Costa, I.A., Barriga, F.J., and Fouquet, Y., 2014, The role of siliceous hydrothermal breccias in the genesis of volcanic massive sulphide deposits—ancient and recent systems: Abstract ID V21A-4737 presented at the 2014 Fall Meeting, AGU, San Francisco, California, 15–19 December.

Cox, S.F., and Munroe, S.M., 2016, Breccia formation by particle fluidization in fault zones: Implications for transitory, rupture-controlled fluid flow regimes in hydrothermal systems: American Journal of Science, v. 316, no. 3, p. 241–278, https://doi.org/10.2475/03.2016.02.

Decandia, F.A., 1982, Geologia dei monti di Spoleto (provincia di Perugia): Bollettino della Società Geologica Italiana, v. 101, p. 291–315.

Dragoni, W., and Verdacchi, A., 1990, First results from the monitoring system of the karstic complex "Grotte di Frasassi-grotta Grande del Vento" (Central Apennines, Italy), *in* Gunay, G., Johnson, A.I., and Back, W., eds., Hydrogeological Processes in Karst Terranes: Proceedings of the Antalya Symposium and Field Seminar: IAHS Publication, v. 207, p. 107–117.

Ergun, S., 1952, Fluid flow through packed columns: Chemical Engineering Progress, v. 48, no. 2, p. 89–94.

Fournier, R.O., 1999, Hydrothermal processes related to movement of fluid from plastic into brittle rock in the magmatic-epithermal environment: Economic Geology, v. 94, no. 8, p. 1193–1211, https://doi.org/10.2113/gsecongeo.94.8.1193.

Frenzel, M., and Woodcock, N.H., 2014, Cockade breccia: Product of mineralization along dilational faults: Journal of Structural Geology, v. 68, p. 194–206, https://doi.org/10.1016/j.jsg.2014.09.001.

Gabitto, J., and Tsouris, C., 2008, Drag coefficient and settling velocity for particles of cylindrical shape: Powder Technology, v. 183, p. 314–322, https://doi.org/10.1016/j.powtec.2007.07.031.

Gidaspow, D., 1994, The fluidized state, *in* Gidaspow, D., ed., Multiphase Flow and Fluidization: Academic Press, p. 97–114.

Giorgioni, M., Tiraboschi, D., Erba, E., Hamann, Y., Weissert, H., and Robinson, S., 2017, Sedimentary patterns and palaeoceanography of the Albian Marne a Fucoidi Formation (Central Italy) revealed by high-resolution geochemical and nannofossil data: Sedimentology, v. 64, no. 1, p. 111–126, https://doi.org/10.1111/sed.12288.

Grare, A., Lacombe, O., Mercadier, J., Benedicto, A., Guilcher, M., Trave, A., Ledru, P., and Robbins, J., 2018, Fault zone evolution and development of a structural and hydrological barrier: the quartz breccia in the Kiggavik Area (Nunavut, Canada) and its control on uranium mineralization: Minerals, v. 8, p. 319–337, https://doi.org/10.3390/min8080319.

Groshong, R.H., Jr., 1975, Strain, fractures, and pressure solution in natural single-layer folds: Geological Society of America Bulletin, v. 86, p. 1363–1376, https://doi.org/10.1130/0016-7606(1975)86<1363:SFAPSI>2.0.CO;2.

Guerrera, F., Tramontana, M., Donatelli, U., and Serrano, F., 2012, Space/time tectono-sedimentary evolution of the Umbria-Romagna-Marche Miocene

Basin (Northern Apennines, Italy): A foredeep model: Swiss Journal of Geosciences, v. 105, p. 325–341, https://doi.org/10.1007/s00015-012-0118-0.

Hunt, J.A., Baker, T., and Thorkelson, D.J., 2005, Regional-scale Proterozoic IOCG-mineralized breccia systems: Examples from the Wernecke Mountains, Yukon, Canada: Mineralium Deposita, v. 40, p. 492–514, https://doi.org/10.1007/s00126-005-0019-5.

Hunt, J.A., Baker, T., Cleverley, J., Davidson, G.J., Fallick, A.E., and Thorkelson, D.J., 2011, Fluid inclusion and stable isotope constraints on the origin of Wernecke Breccia and associated iron oxide–copper–gold mineralization, Yukon: Canadian Journal of Earth Sciences, v. 48, p. 1425–1445, https://doi.org/10.1139/e11-044.

Imber, J., Holdsworth, R.E., and Butler, C.A., 2001, A reappraisal of the Sibson-Scholz fault zone model: The nature of the frictional to viscous ("brittle-ductile") transition along a long-lived, crustal-scale fault, Outer Hebrides, Scotland: Tectonics, v. 20, no. 5, p. 601–624, https://doi.org/10.1029/2000TC001250.

Jébrak, M., 1997, Hydrothermal breccias in vein-type ore deposits: A review of mechanisms, morphology and size distribution: Ore Geology Reviews, v. 12, p. 111–134, https://doi.org/10.1016/S0169-1368(97)00009-7.

Jébrak, M., Marcoux, E., and Fontaine, D., 1996, Hydrothermal silica–gold stalactites formed by colloidal deposition in the Cirotan epithermal deposit, Indonesia: Canadian Mineralogist, v. 34, p. 931–938.

John, D.A., Vikre, P.G., du Bray, E.A., Blakely, R.J., Fey, D.L., Rockwell, B.W., Mauk, J.L., Anderson, E.D., and Graybeal, F.T., 2018, Descriptive models for epithermal gold-silver deposits: U.S. Geological Survey Scientific Investigations Report 2010-5070-Q, 247 p., https://doi.org/10.3133/sir20105070Q.

Jordan, J.S., Hesse, M.A., and Rudge, J.F., 2018, On mass transport in porosity waves: Earth and Planetary Science Letters, v. 485, p. 65–78, https://doi.org/10.1016/j.epsl.2017.12.024.

Kalliokoski, J., and Rehn, P., 1987, Geology of the veins and vein sediments of the Golden Wonder Mine Lake City, Colorado: An epithermal hot springs gold-alunite deposit, U.S. Geological Survey Open File Report, 87-344, 47 p.

Kellermeier, M., Glaa, F., Klein, R., Melero-Garcıa, E., Kunz, W., and Garcıa-Ruiz, J.M., 2013, The effect of silica on polymorphic precipitation of calcium carbonate: An on-line energy-dispersive X-ray diffraction (EDXRD) study: Nanoscale, v. 5, p. 7054–7065, https://doi.org/10.1039/c3nr00301a.

Kusznir, N.J., and Park, R.G., 1986, Continental lithosphere strength: The critical role of lower crustal deformation: Geological Society, London, Special Publications, v. 24, p. 79–93, https://doi.org/10.1144/GSL.SP.1986.024.01.09.

Ladeira, F.L., and Price, N.J., 1981, Relationship between fracture spacing and bed thickness: Journal of Structural Geology, v. 3, no. 2, p. 179–183, https://doi.org/10.1016/0191-8141(81)90013-4.

Lakshtanov, L.Z., and Stipp, S.L.S., 2010, Interaction between dissolved silica and calcium carbonate: 1. Spontaneous precipitation of calcium carbonate in the presence of dissolved silica: Geochemica et Cosmochimica Acta, v. 74, p. 2655–2664.

Laughton, J.R., Thorkelson, D.J., Brideau, M.A., Hunt, J.A., and Marshall, D.D., 2005, Early Proterozoic orogeny and exhumation of Wernecke Supergroup revealed by vent facies of Wernecke Breccia, Yukon, Canada: Canadian Journal of Earth Sciences, v. 42, p. 1033–1044, https://doi.org/10.1139/e04-085.

Loorents, K.J., Björklund, L., and Stigh, J., 2000, Effect of induced fracturing based on a natural fracture system in a dimension stone quarry in the Offerdal Nappe, Sweden: Bulletin of Engineering Geology and the Environment, v. 58, p. 215–225, https://doi.org/10.1007/s100640050077.

Lugli, S., 2001, Timing of post-depositional events in the Burano Formation of the Secchia Valley (Upper Triassic, Northern Apennines), clues from gypsum-anhydrite transitions and carbonate metasomatism: Sedimentary Geology, v. 140, p. 107–122, https://doi.org/10.1016/S0037-0738(00)00174-3.

Mirabella, F., Ciaccio, M.G., Barchi, M.R., and Merlini, S., 2004, The Gubbio normal fault (Central Italy): Geometry, displacement distribution and tectonic evolution: Journal of Structural Geology, v. 26, p. 2233–2249, https://doi.org/10.1016/j.jsg.2004.06.009.

Mitelman, A., and Elmo, D., 2014, Modelling of blast-induced damage in tunnels using a hybrid finite-discrete numerical approach: Journal of Rock Mechanics and Geotechnical Engineering, v. 6, p. 565–573, https://doi.org/10.1016/j.jrmge.2014.09.002.

Molli, G., Crispini, L., Malusa, M., Mosca, P., Piana, F., and Federico, L., 2010, Geology of the Western Alps-Northern Apennine junction area: A regional review, *in* Beltrando, M., Peccerillo, A., Mattei, M., Conticelli, S., and Doglioni, C., eds., The Geology of Italy: Tectonics and life along plate margins: Journal of the Virtual Explorer, v. 36, paper 10, https://doi.org/10.3809/jvirtex.2010.00215.

Montanari, A., Chan, L.S., and Alvarez, W., 1989, Synsedimentary tectonics in the Late Cretaceous–Early Tertiary pelagic basin of the Northern Apennines, Italy, *in* Crevello, P.D., Wilson, J.L., Sarg, J.F., and Read, J.F., eds., Controls on Carbonate Platforms and Basin Development: Society for Sedimentary Geology (SEPM) Special Publication 44, p. 379–399, https://doi.org/10.2110/pec.89.44.0379.

Mort, K., and Woodcock, N.H., 2008, Quantifying fault breccia geometry: Dent Fault, NW England: Journal of Structural Geology, v. 30, p. 701–709, https://doi.org/10.1016/j.jsg.2008.02.005.

Müller, A., Ganerød, M., Wiedenbeck, M., Olaus, S., Spjelkavik, S., and Selbekk, R., 2018, The hydrothermal breccia of Berglia-Glassberget, Trøndelag, Norway: snapshot of a Triassic earthquake: Minerals, v. 8, no. 5, p. 175, https://doi.org/10.3390/min8050175.

Oliver, N.H.S., Rubenach, M.J., Fu, B., Baker, T., Blenkinsop, T.G., Cleverley, J.S., Marshall, L.J., and Ridd, P.J., 2006, Granite-related overpressure and volatile release in the mid crust: Fluidized breccias from the Cloncurry District, Australia: Geofluids, v. 6, p. 346–358, https://doi.org/10.1111/j.1468-8123.2006.00155.x.

Ollier, C.D., 2007, Breccia-filled pipes: distinguishing between volcanic and non-volcanic origins: Geografia Fisica e Dinamica Quaternaria, v. 30, p. 63–76.

Patrício, M., and Mattheij, R.M.M., 2007, Crack propagation analysis: Eindhoven, Technische Universiteit Eindhoven, CASA report, v. 723, 22 p.

Peacock, D., Rotevatn, A., and Sanderson, D.J., 2019, Brecciation driven by changes in fluid column heights: Terra Nova, v. 31, no. 1, p. 76–81, https://doi.org/10.1111/ter.12371.

Petrie, E.S., Jeppson, T.N., and Evans, J.P., 2012, Predicting rock strength variability across stratigraphic interfaces in caprock lithologies at depth: Correlation between outcrop and subsurface: Environmental Geoscience, v. 19, no. 4, p. 125–142, https://doi.org/10.1306/eg.06011212001.

Quinn, H.M., 2014, A reconciliation of packed column permeability data: Deconvoluting the Ergun papers: Journal of Materials, Article ID 548482, 24 p., https://doi.org/10.1155/2014/548482.

Rowe, K.J., and Rutter, E.H., 1990, Palaeostress estimation using calcite twinning: Experimental calibration and application to nature: Journal of Structural Geology, v. 12, no. l, p. 1–17, https://doi.org/10.1016/0191-8141(90)90044-Y.

Saharan, M.R., Mitri, H.S., and Jethwa, J.L., 2006, Rock fracturing by explosive energy: Review of state-of-the-art: Fragblast, v. 10, no. 1–2, p. 61–81, https://doi.org/10.1080/13855140600858792.

Santantonio, M., and Carminati, E., 2011, Jurassic rifting evolution of the Apennines and Southern Alps (Italy): Parallels and differences: Geological Society of America Bulletin, v. 123, no. 3–4, p. 468–484, https://doi.org/10.1130/B30104.1.

Scheepers, R., and Cuney, M., 1992, Hydrothermal breccia-related Cu-Mo-Au mineralization in Late Precambrian granites, Western Cape Province, South Africa: Ore Geology Reviews, v. 7, p. 1–23.

Scholz, C.H., 1988, The brittle-plastic transition and the depth of seismic faulting: Geologische Rundschau, v. 77, no. 1, p. 319–328, https://doi.org/10.1007/BF01848693.

Scisciani, V., Tavarnelli, E., and Calamita, F., 2001, Styles of tectonic inversion within syn-orogenic basins: Examples from the Central Apennines, Italy: Terra Nova, v. 13, p. 321–326, https://doi.org/10.1046/j.1365-3121.2001.00352.x.

Scuderi, M.M., Kitajima, H., Carpenter, B.M., Saffer, D.M., and Marone, C., 2015, Evolution of permeability across the transition from brittle failure to cataclastic flow in porous siltstone: Geochemistry Geophysics Geosystems, v. 16, no. 9, p. 2980–2993, https://doi.org/10.1002/2015GC005932.

Shukla, M.K., and Sharma, A., 2018, A brief review on breccia: it's contrasting origin and diagnostic signatures: Solid Earth Sciences, v. 3, p. 50–59, https://doi.org/10.1016/j.sesci.2018.03.001.

Sibson, R.H., 1977, Fault rocks and fault mechanisms: Journal of the Geological Society, London, v. 133, p. 191–213, https://doi.org/10.1144/gsjgs.133.3.0191.

Sibson, R.H., 1981, Fluid flow accompanying faulting: Field evidence and models, *in* Simpson, D.W., and Richards, P.G., eds., Earthquake Prediction:

An International Review, volume 4: AGU, Maurice Ewing Series, p. 593–603, https://doi.org/10.1029/ME004p0593.

Sibson, R.H., 1986, Brecciation processes in fault zones: Inferences from earthquake rupturing: Pure and Applied Geophysics, v. 124, p. 159–175, https://doi.org/10.1007/BF00875724.

Sibson, R.H., 1996, Structural permeability of fluid-driven fault fracture meshes: Journal of Structural Geology, v. 18, p. 1031–1042, https://doi.org/10.1016/0191-8141(96)00032-6.

Sibson, R.H., Moore, J.McM., and Rankin, A.H., 1975, Seismic pumping—a hydrothermal fluid transport mechanism: Journal of the Geological Society, London, v. 131, p. 653–659, https://doi.org/10.1144/gsjgs.131.6.0653.

Sutarto, S., Idrus, A., Harijoko, A., Setijadji, L.D., and Meyer, F.M., 2015, Veins and hydrothermal breccias of the Randu Kuning porphyry CU-AU and epithermal AU deposits at Selogiri area, Central Java Indonesia: Journal of Applied Geology, v. 7, no. 2, p. 82–101, https://doi.org/10.22146/jag.26982.

Tămaș, C.G., and Milési, J.P., 2002, Hydrovolcanic breccia pipe structures—general features and genetic criteria: I. Phreatomagmatic breccias: Studia Universitatis Babeș Bolyai Geologia, v. 47, p. 127–147, https://doi.org/10.5038/1937-8602.47.1.10.

Tavarnelli, E., 1996, The effects of pre-existing normal faults on thrust ramp development: an example from the Northern Apennines, Italy: Geologische Rundschau, v. 85, p. 363–371, https://doi.org/10.1007/BF02422241.

Tavarnelli, E., and Peacock, D.C.P., 1999, From extension to contraction in syn-orogenic foredeep basins: the Contessa section, Umbria-Marche Apennines, Italy: Terra Nova, v. 11, p. 55–60, https://doi.org/10.1046/j.1365-3121.1999.00225.x.

Tognaccini, S., Tavarnelli, E., and Montanari, A., 2019, Synsedimentary deformation in Upper Cretaceous–Lower Paleogene limestones within a thrust anticline of the Umbria-Marche Apennines, Italy, *in* Koeberl, C., and Bice, D.M., eds., 250 Million Years of Earth History in Central Italy: Celebrating 25 Years of the Geological Observatory of Coldigioco: Geological Society of America Special Paper 542, p. 213–228, https://doi.org/10.1130/2019.2542(11).

Valverde, J.M., 2015, Dynamical weakening by fluidization under oscillatory viscous flows: Journal of Geophysical Research: Solid Earth, v. 120, no. 11, p. 7641–7654, https://doi.org/10.1002/2015JB011972.

Wenrich, K.J., 1985, Mineralisation of breccia pipes in Northern Arizona: Economic Geology, v. 80, p. 1722–1735, https://doi.org/10.2113/gsecongeo.80.6.1722.

Woodcock, N.H., and Mort, K., 2008, Classification of fault breccias and related fault rocks: Geological Magazine, v. 145, no. 3, p. 435–440, https://doi.org/10.1017/S0016756808004883.

Yang, S., Danek, T., Cheng, X., and Huang, Q., 2017, Review of carbonate breccia genetic classification in West Hill, Beijing: IOP Conference Series: Earth and Environmental Science, v. 95, https://doi.org/10.1088/1755-1315/95/2/022050.

Zhang, Y., Zhang, S., and Pirajn, F., 2007, Fluidization: an important process in the formation of the Qiyugou Au-bearing breccia pipes in Central China: Acta Geologica Sinica, v. 81, v. 2, p. 226–238.

Zheng, J., and Hryciw, R.D., 2015, Traditional soil particle sphericity, roundness and surface roughness by computational geometry: Geotechnique, v. 65, no. 6, p. 494–506, https://doi.org/10.1680/geot.14.P.192.

Zielke, O., Mai, M., and Schorlemmer, D., 2018, Postseismic deepening of the brittle-ductile transition zone depth: Geophysical Research Abstracts, EGU General Assembly, Proceedings of EGU2018, 4–13 April, Vienna, Austria, p. 2362.

Manuscript Accepted by the Society 4 October 2021
Manuscript Published Online 2 March 2022

Printed in the USA